Int. J. Electrochem. Sci., 8 **(2013)** 3357 - 3370

International Journal of
ELECTROCHEMICAL
SCIENCE
www.electrochemsci.org

Determination of Equivalent Circuit Parameters of a Contactless Conductive Detector in Capillary Electrophoresis by an Impedance Analysis Method

Zhenli Zhang[1,2], Yaolong Li[1], Zhongshi Xu[1], Xilei Zhu[1], Qi Kang[1], Dazhong Shen[1,3*]*

[1]The Key Lab in Molecular and Nano-materials Probes of the Ministry of Education of China, College of Chemistry, Chemical Engineering and Materials Science, Shandong Normal University, Jinan, 250014, P.R. China.
[2]Zibo Institute of Product Quality Supervision & Inspection, Zibo, 250063, P.R.China
[3]Key Laboratory of Chemical Biology and Traditional Chinese Medicine Research (Hunan Normal University), Ministry of Education, Changsha,410081, P.R.China
[*]E-mail: qikang@sdu.edu.cn;dzshen@sdnu.edu.cn;

Received: 29 December 2012 / *Accepted:* 6 February 2013 / *Published:* 1 March 2013

The equivalent circuit parameters of a capacitively coupled contactless conductive detector (C^4D) were measured by an impedance analysis method. The change in the equivalent circuit parameters was explained by an electrical line distribution model. It was shown that the total impedance of a C^4D under capillary electrophoresis conditions is composed mainly of the impedance from the wall capacitor (C_W). The value of C_W is much less than that predicted from a cylinder capacitor model. With increasing solution conductivity in the capillary, the value of C_W increases. As the electrode length increases, C_w increases and attains to a plateau value. The effective electrode length is obviously less than its geometrical length. As the operating frequency increases, the value of C_w reduces dramatically. The response of a C^4D is due to the changes in both of C_w and solution resistance.

Keywords: Contactless conductivity detector; Capillary electrophoresis; Impedance analysis, Equivalent circuit parameter

1. INTRODUCTION

Since the work of Zemann et al. [1] and da Silva and do Lago [2] in 1998, a capacitively coupled contactless conductive detector (C^4D) has received considerable attention as an alternative and universal detection method to determine the charged species that are not suitable for the common UV absorbance detection in capillary and microchip electrophoresis [3-8]. In the construction of C^4D, the sensing electrodes are not in a direct contact with the electrolyte, which presents a more robust and

easy handle alternative to the contact conductivity method. The applications of C^4D were reported in high-performance liquid chromatography [9,10], ion chromatography [11,12] and flow injection analysis [13], non-invasive characterization of monolithic stationary-phase coatings [14,15], measurement of electroosmotic flow [16], and conductivity of aqueous droplets in segmented flow[17].

A C^4D makes use of two sensing electrodes placed in close proximity to a microchannel where detection is performed. An alternating actuator voltage is applied to the input electrode and coupled capacitively through the solution in microchannel to signal electrode. The pick-up current is subsequently detected as the response signal of C^4D in a chromatogram. The theoretical aspects related to the response of C^4D are helpful to show how the detector can be optimized further. The equivalent electrical models were reported to describe the response of C^4D [2,18,19]. The influences of the factors such as operating frequency [20-22], excitation voltage [23], detection cell geometry [24], wall thickness of capillary [25], stray capacitance [26,27], and design of detection system [28] on the response of C^4D were investigated. To our best knowledge, the measurement of equivalent circuit parameters of C^4D under capillary electrophoresis conditions has not been reported.

In this work, the equivalent circuit parameters of C^4D were measured by an impedance analysis method. The influences of solution conductivity, operating frequency, electrode length and electrode gap size on the wall capacitance (C_W), solution resistance (R_S) and solution capacitance (C_S) of C^4D were investigated. The changes in these parameters were analyzed by an electrical line distribution model.

2. EXPERIMENTAL

2.1. Reagents and instrumentation

A schematic representation of the experimental setup for impedance measurement of C^4D is presented in Fig.1.

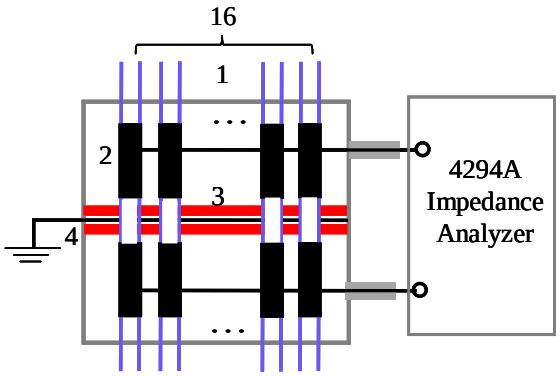

Figure 1. Schematic illustration of C^4D array for impedance measurement (not to scale). (1): capillary array; (2): contactless electrode; (3): Teflon insulation film; (4): ground shielding plate and box.

Fused silica capillary (with inter diameter of 50 μm, outside diameter of 325 μm and thickness of polyimide-coated layer of 20 μm) was production of Yongnian Optical Fiber Factory (Hebei, China). The contactless electrodes were fabricated from syringe cannulas of a given length (1-18 mm). The gap size between the input and signal electrodes was measured by a magnifying glass provided with a scale. To increase the signal-to-noise ratio in impedance data, the parallel array of 16 C^4Ds with the same electrode geometry was employed and set in a grounded shielding box. A grounded copper plate (thickness of 0.5 mm) was mounted between the input and signal electrodes to minimize the stray capacitance. Sixteen holes (with diameter of 0.45 mm) were bored in the copper plate and Teflon insulation film (thickness of 0.2 mm) to pass the array of capillary. Impedance measurements were performed in an impedance analyzer (Model 4294A, Agilent) at the constant laboratory temperature of 25 ± 1°C. A user program written in Visual Basic 6.0 was used to acquire and process the impedance data. The averaged admittance data were divided by 16 and used to calculate the equivalent circuit parameters in a single C^4D.

All chemicals were of reagent grade and deionized water (Millipore, Bedford, MA, USA) was used throughout. All solutions were degassed by ultrasonication and filtered through 0.2 μm nylon syringe filters prior to use.

2.2 Measurement of the equivalent circuit parameters in an impedance analysis method.

Prior to measurement, the impedance analyzer was calibrated at given measuring frequency region. The capillary array was flushed with 0.1 M NaOH for 3 min, deionized water for 5 min and acetone for 3 min, and dried by passage of nitrogen stream for 10 min. The residual capacitance of the C^4D array with dry capillaries was measured and recorded as the leakage capacitance (C_0). The capillary array was filled with KCl solution of given specific conductivity. The conductance (G) and susceptance (B) of the C^4D array were scanned. The averaged values of G and B at each frequency in ten repetitive measurements were recorded. The equivalent circuit parameters of C^4D in Fig.2A were

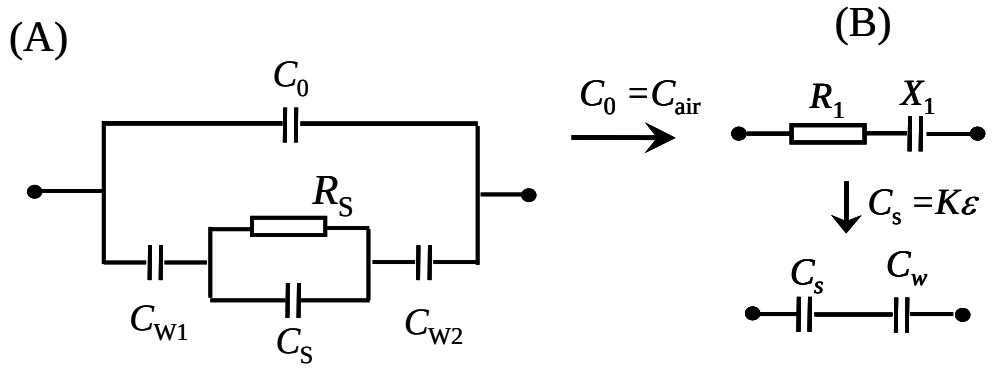

Figure 2. (A): Simplified equivalent circuit model of C^4D; (B): parameters calculation processes in impedance analysis method. Where C_0 and C_W are the leakage capacitance and wall capacitance, R_S and C_S are the solution resistance and solution capacitance, respectively. R_1 and X_1 are the total series resistance and inductance of the C^4D after correction of C_0, respectively.

estimated by the method discussed in section 3.1. When the solution in capillary array was replaced by another test solution, the equivalent circuit parameters of C^4D in a new solution were measured again.

3. RESULTS AND DISCUSSION

3.1 Estimation of the equivalent circuit parameters of C^4D by impedance analysis method

Analysis of the equivalent circuit of C^4D is helpful to optimize detector. Figs.2A depicts a typical simplified equivalent circuit model for C^4D [2,18,19,29,30]. Accordingly, the admittance of C^4D, Y, is expressed by:

$$Y = G + iB = \frac{G_S}{\alpha^2 + (1+\beta)^2} + i\left[\omega(C_0 + C_W) - \frac{\omega(C_S + C_W)}{\alpha^2 + (1+\beta)^2}\right] \qquad (1)$$

where $G_S=1/R_S=K\kappa$, $C_s=K\varepsilon_0\varepsilon_r$, C_S and G_S are the solution capacitance and conductance, K is the cell constant, κ and ε_r are the specific conductivity and relative dielectric constant of the test solution, $\varepsilon_0=8.854\times10^{-12}$ F/m, respectively. And $C_W= C_{W1}C_{W2}(C_{W1}+C_{W2})^{-1}$, is the total series wall capacitance in C^4D, $\alpha = (R_S\ \omega C_W)^{-1}$, is the ratio of capacitive impedance from capillary wall to solution resistance, $\beta=C_S/C_W$, is the ratio of solution capacitance to wall capacitance, $i=\sqrt{-1}$ is the imaginary unit, respectively.

In the parallel arrangement measurement model, the real part (G) and imaginary part (B) of a combination of electrical elements (C^4D in this work) were measured simultaneously at a given frequency in an impedance analyzer. As can be seen in Eq.(1), the values of G and B are related to three and four elements in Fig.2A, respectively. In order to understand the electrical response of C^4D, it is necessary to calculate these equivalent circuit parameters by using the values of G and B measured in an impedance analysis method.

As shown in Fig.2A, C_0 is in a parallel arrangement with the series branch of solution and wall impedance. When the capillary array was dried by a nitrogen stream, the series branch through solution is assumed to cut off because the high impedance from the dry channels in capillaries. Hence, the value of C_0 in C^4D was measured directly in such situation. Under our experimental conditions, the value of C_0 in a single C^4D is in the range of 0.08-0.26 fF in the frequency range from 50 kHz to 5 MHz. Because the value of C_0 is related to the shielding conditions, iIt is difficult to compare its value in different C^4D designs. On the other hand, the value of C_0 is small under well designed shielding conditions. Hence, the change in C_0 is not discussed in this work.

When the capillaries were filled with a test solution, the contribution of C_0 to the value of B is corrected by: $B_1=B-\omega C_0$, where $\omega=2\pi f$, f is the measuring frequency. Accordingly, the total impedance of the series arrangement of solution and wall impedance is obtained and presented by a resistance of R_1 and reactance of X_1 in series (Fig.2B). The values of R_1 and X_1 are calculated by the following equations:

$$R_1 = \frac{G}{G^2 + B_1^2} = \frac{\kappa}{K(\kappa^2 + \omega^2\varepsilon^2)} \quad (2)$$

$$X_1 = -\frac{B_1}{G^2 + B_1^2} = -\frac{1}{\omega C_w} - \frac{\omega C_s}{G_s^2 + \omega^2 C_s^2} \quad (3)$$

Based on Eq.(2), the cell constant (K) is estimated firstly by using the known solution conductivity and dielectric constant (ε_r=78). Afterward, the values of G_S, C_S and R_S are calculated from the values of K,κ and ε_r. Finally, the value of C_W is calculated by the following equation.

$$C_w = \left(\frac{\omega B_1}{G^2 + B_1^2} - \frac{\omega^2 C_s}{G_s^2 + \omega^2 C_s^2} \right)^{-1} \quad (4)$$

Thus, the four equivalent circuit parameters of C^4D in Fig.2A are estimated by the proposed impedance analysis method.

3.2 Influence of solution conductivity on R_S in C^4D

Usually, the value of R_S is expressed as:

$$R_S = \frac{1}{G_S} = \frac{d}{\pi r_1^2 \kappa} \quad (5)$$

where d is the electrode gap size, r_1 is the radius of the microchannel in capillary, respectively.

The dependence of R_S on solution conductivity is shown in Fig.3. As expected, R_S decreases near-linearly with increasing κ in the figure under dual-logarithmic coordinates. However, the value of R_S deviates the predication from Eq.(5) if the geometrical electrode gap is used, especially in the C^4D with a short electrode gap. In the C^4Ds with d = 1.1 mm and d = 2.0 mm, for example, the values of R_S are less than the predictions by Eq.(5) in solutions with κ<0.04 S/m and κ<0.06 S/m, respectively. But a contrary case was observed in solutions of higher conductivity. As reported previously [21], the resistance values obtained from the Bode plots are slightly higher than the resistance values calculated by Eq.(5). They concluded that the actual cell resistance is not completely determined by the solution between the ends of the electrodes but to a small extent also by the volume inside each electrode. As the electrode gape size increases, the value of R_S increases. The values of R_S in the C^4D with d = 4.2 are close to the predictions. In the C^4Ds with d = 7.8 mm and d = 16 mm, the values of R_S are less than the predictions in the solutions tested. On the other hand, a decrease in solution capacitance with increasing conductivity is observed in C^4D with a given gap (data is not shown).

3.3 Influence of solution conductivity on C_W in C^4D

Based on a cylinder capacitor model [19, 21,24, 31], the value of C_{W1} (or C_{w2}) is predicted by the following equation:

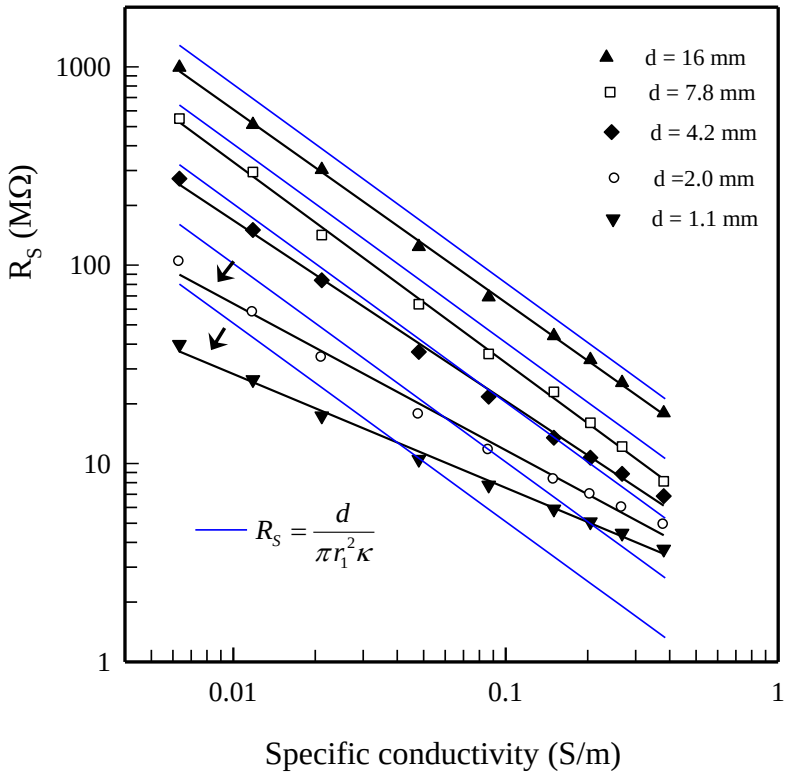

Figure 3. Influence of the solution conductivity on the solution resistance in C^4D with different gap sizes . Other conditions: L=18 mm, f =200 kHz.

$$C_{w1} = \frac{2\pi L \varepsilon_0 \varepsilon_r}{\ln(r_2 / r_1)} \qquad (6)$$

where L is the electrode length, r_2 is the outer diameter of the capillary, ε_r is the relative permittivity of wall, respectively. By using the values of L=18 mm, r_1=50 μm, r_2=375 μm and ε_r=4.4 (quartz) under our experimental conditions, there should be C_w =1.1 pF (C_{w1}= C_{w2}) in all test solutions.

As shown in Fig.4, however, the value of C_W is much less than this predication (1.1 pF), especially in solutions of low conductivity. For example, the C_W values measured in C^4D (d =1.1 mm) in 1 and 30 mM KCl solutions are 13.4 and 103 *f*F, which is about 1.24% and 9.4% of the predication. In addition, the value of C_W increases near-linearly with increasing solution conductivity. As the electrode gap size increases, the value of C_W decreases further.

To explore the discrepancy between the values measured and predicated, the value of C_W was calculated by a more precise way. In fact, the value of C_{w1} or C_{w2} in C^4D is related to four equivalent capacitors with different dielectric materials, i.e., air capacitor between the contactless electrode and polyimide layer (C_1), polyimide layer capacitor (C_2), quartz wall capacitor (C_3) , and double-layer capacitor at quartz/solution interface (C_4). Under our experimental conditions, the inter diameter of the syringe cannula is 400 μm, we have C_1 = 15.5 pF by using the values of L=18 mm, r_1=375 μm, r_2=400 μm and ε_r =1 (air). As the thickness of the polyimide-coated layer (ε_r =3.5) is 20 μm, there are r_1=325

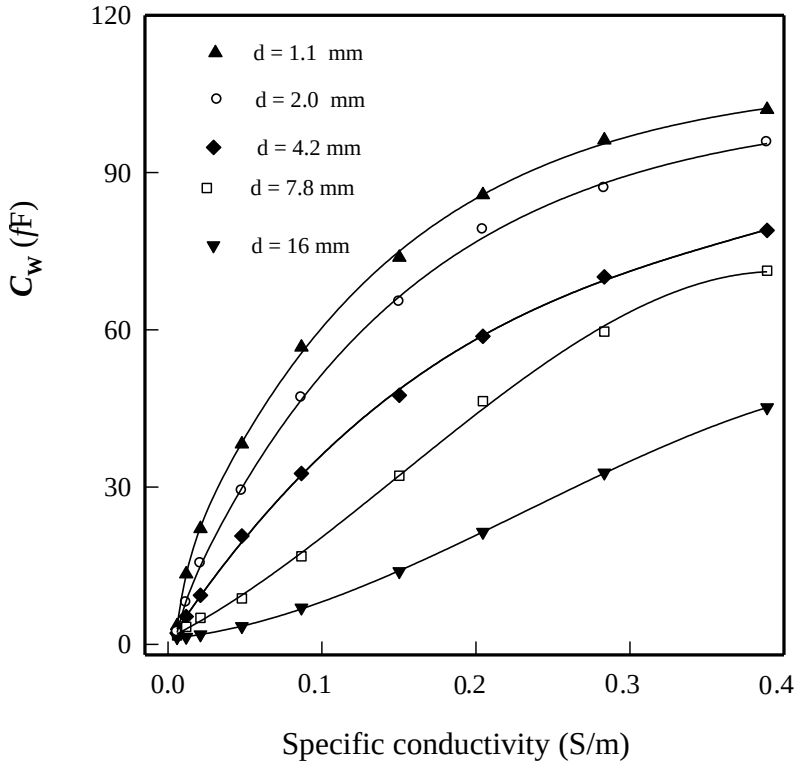

Figure 4. Influence of the solution conductivity on the wall capacitance in C^4D with different gap sizes. Other conditions: L=18 mm, f =200 kHz.

μm, r_2=375 μm and C_2=24.5 pF. Similarly, the capacitance from quartz wall (r_1=50 μm, r_2=325 μm) is C_3=2.35 pF. As the double-layer capacitor at solid/solution interface is in the order of 0.1-10 μF/cm^2, the value of C_4 (2-200 nF), which is much lager than C_1, C_2 and C_3. The total series capacitance of the four equivalent capacitors is equal to 1.88 pF. The new predicted value of C_W = 0.94 pF in C^4D is still much larger than the measured values.

To explain the discrepancy between the values of C_W measured and predicated, a simplified electrical line distribution model in Fig.5 is proposed in this work. When the capillary is filling by solution of low conductivity, the electrical lines from electrode to solution are not perpendicular to the capillary, the passing distance of the electrical lines is larger than the thickness of capillary (Fig.5A). Hence, the value of C_W is less than the predication according to a cylinder capacitor model. With increasing solution conductivity, the width of the detection zone (between the electrodes to pass through the electrical lines) increases, which is supported by the decrease in C_S. The angles between the electrode and electrical lines (θ) increase and the distance of the electrical line from the electrode to solution reduces (Fig.5B). Hence, the value of C_W increases with increasing conductivity. In the work of Kubáň and Hauser [21], the experimental values of C_W were about 4 times smaller than the calculated ones. They ascribed the discrepancy to the fact that the electrolyte solution inside the capillary is not a metallic conductor of low resistance as assumed by the model. When the capillaries were filled with mercury as an extreme case of high conductivity, the electrical lines are perpendicular to the capillary (Fig.5C). The passing distance of the electric lines from electrode to solution is equal to

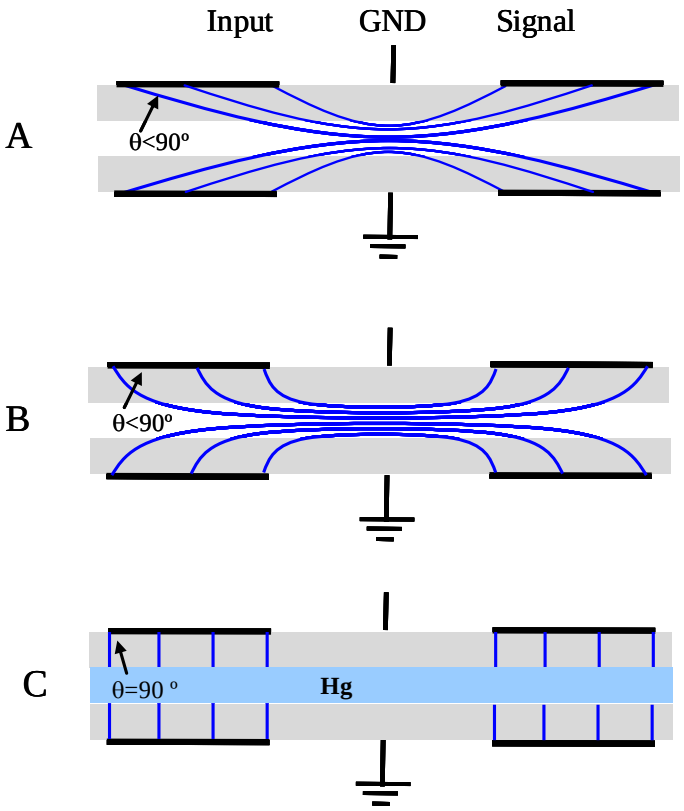

Figure 5. Simplified illustration for electrical line distribution models in C^4D under different situations (not to scale). (A): filled by solution of low conductivity; (B): filled by solution of high conductivity ; (C): filled by mercury.

the thickness of capillary wall. The value of C_W =1.05 pF was measured, which is close to the predication because the cylinder capacitor model is holden in such case.

According to the model in Fig.5A, with increasing electrode gap size, the passing distance of the electrical lines from electrode to solution increases, hence, the value of C_W reduces.

3.4 Influence of electrode length on C_W , C_S and R_S in C^4D

As mentioned above, the value of C_W measured is much less than the predication, which reveals that the effective electrode length is less than its geometrical length [24]. The dependence of C_W on electrode length shown in Fig.6A supports this conclusion further. With increasing electrode length, the value of C_W increases and attains to a plateau value. This result is explained by the electrical line distribution model in Fig.5A. Under our experimental conditions, the electrode length is much larger than the inner diameter of capillary, i.e., $L>>r_1$. The distribution of electrical lines is limited by the cross area of solution in capillary. Because the outside ring area near the capillary wall is occupied preferentially by the electrical lines from the inside end of the electrode, electrical lines from the outer segment of the electrode are blocked by that from the inner one. They have to pass through the inner ring region with less conducting area and longer distance. Thus, the segment of the electrode at outside end has much less contribution for current conduction than that at inside end due to

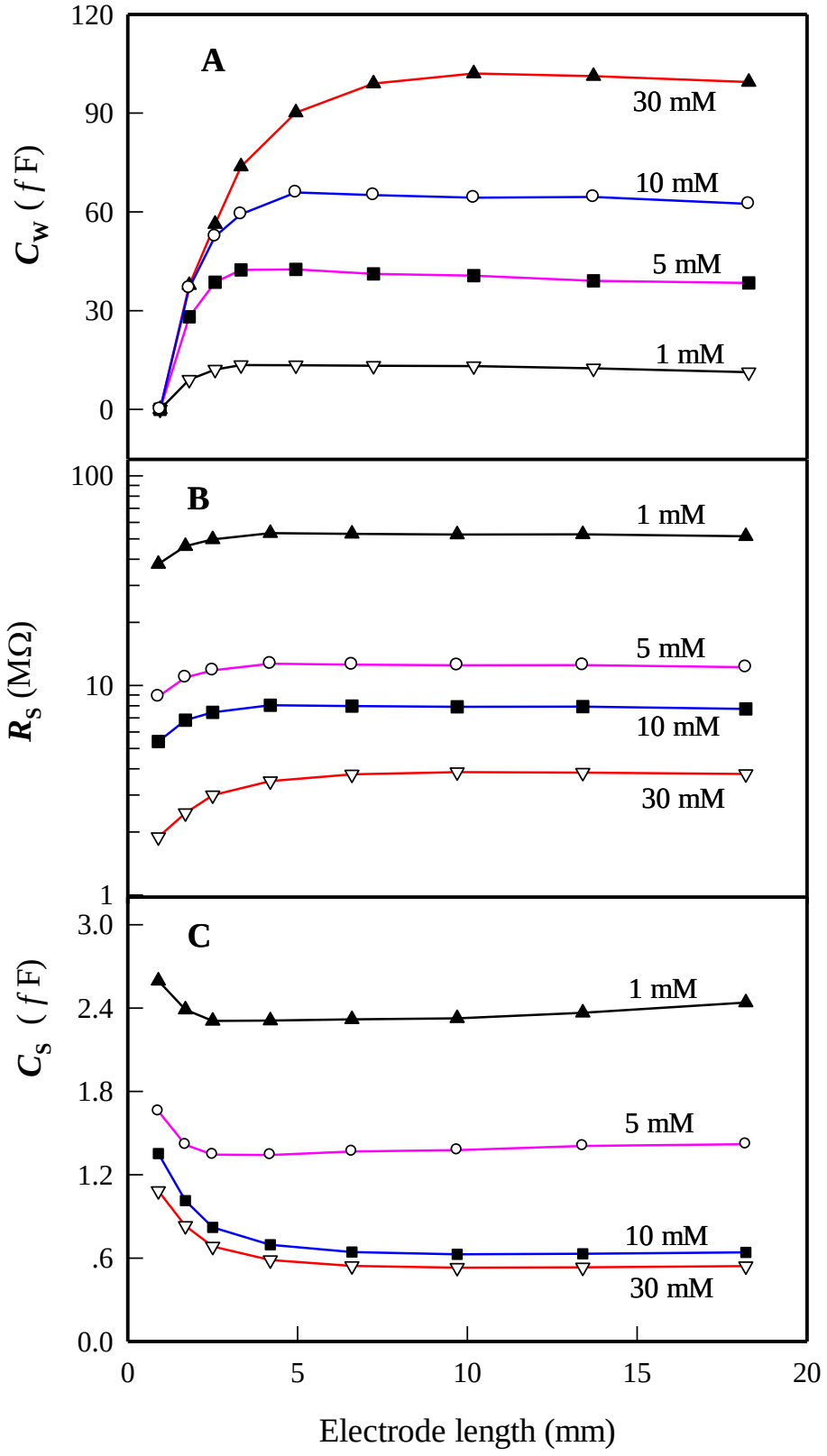

Figure 6. Influence of electrode length on wall capacitance (A),solution resistance (B) and solution capacitance (C) in C^4D. Other experimental conditions: d =1.1 mm, f =200 kHz.

a larger solution resistance. Hence, the effective electrode length in C^4D is less than its geometrical length.

The influence of electrode length on solution resistance and solution capacitance in C^4Ds with d =1.1 mm is shown in Figs.6B and 6C. With increasing electrode length, the value of R_S increases while the value of C_S decreases slightly. This result reveals that a wider detection zone occurs in the C^4D with a larger electrode length. It should be noted that the increase in electrode length is helpful to enhance the sensitivity of C^4D due to larger C_W. On the other hand, however, the increase in detection zone length with increasing electrode length corresponds to a larger detection volume, which is disadvantageous for the peak resolution in capillary electrophoresis.

3.5 Influence of operating frequency on C_w and R_s in C^4D

It was shown that the operating frequency is an important factor to influence the response of C^4D [20-22]. Fig.7 illustrates the values of C_W and R_S measured at the frequency range from 50 kHz to 5 MHz, which covers the frequency region reported in references [4,7]. With increasing operating frequency, the effective electrode length in C^4D is reduced [24]. In addition, the detection zone in capillary is thought to be compressed due to the skin effect at high frequency. Hence, C_w reduces dramatically and R_S decreases near-linearly with increasing frequency.

As the signal current in C^4D is proportional to $|Y|$, which stands for the response characteristic of C^4D itself. As shown in Fig.8A, with increasing measuring frequency, the value of $|Y|$ increases until to a maximum then decreases. It was shown that the operating frequency corresponding to the maximum response signal is related to the experimental conditions, including input-signal amplitude [20,32], amplifier[21], cell dimension [33].

To explain the frequency characteristic of C^4D, the values of $\alpha = |X_{Cw}|/Rs = (R_S\ \omega C_w)^{-1}$ were calculated and shown in Fig.8B. It can be seen that the reactance from C_W is larger than the resistance from solution, except in 1 mM KCl solution with f <130 kHz. Under the condition of $C_w >> C_S$ and $C_w >> C_0$ in the region of low frequency, there are $1+\beta \approx 1$ and $1+\gamma \approx 1$ in Eq.(3), the expression of $|Y|$ is simplified as:

$$|Y| \approx \frac{1}{\sqrt{R_S^2 + X_{Cw}^2}} = \frac{1}{R_S\sqrt{1+\alpha^2}} \qquad (7)$$

With increasing frequency, the value of R_S decreases, according to Eq.(7), an increase in $|Y|$ is expected because the change in value of α is slightly (see Fig.8B). In the region of high frequency, the value of α increases with increasing frequency. The value of $|Y|$ is close to $\omega(C_w+C_0)$. In the frequency range from 500 to 5000 kHz, the regressed relation: $\lg C_W = m - n\lg f$ was obtained. The values of n are 1.09, 1.61, 1.48 and 1.27 in 1,5,10 and 30 mM KCl solutions, respectively. Consequently, the value of ωC_w ($\propto f^{1-n}$) decreases as the frequency increases. Because the value of C_W in 1 mM KCl solution is not much larger than C_0, the value of $|Y|$ increases slightly with increasing frequency. On the other hand, as can be seen in Fig.8A, the noise level in the high frequency region is higher than that in low

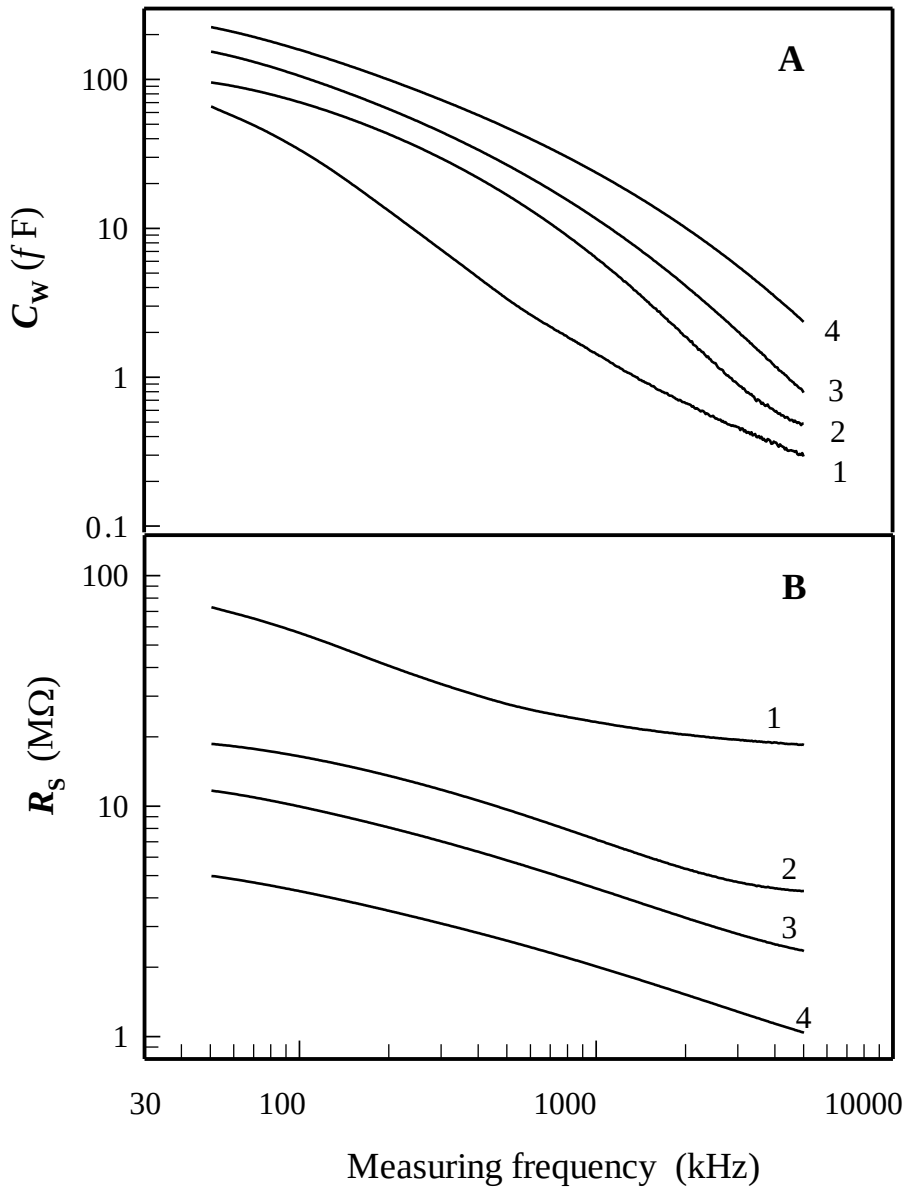

Figure 7. Influence of measuring frequency on the wall capacitance (A) and solution resistance (B) in C^4D. Other experimental conditions: *L*=18 mm, *d* =1.1 mm. KCl concentration: (1): 1 mM; (2): 5 mM; (3): 10 mM; (4): 30 mM.

frequency region due to the much less C_W in the latter, especially in solutions of low conductivity.

It should be noted that only the frequency behavior of C^4D itself is measured in the impedance analyzer. In the applications of C^4D, a simplified detection circuitry is employed due to its much lower cost and higher measurement speed at a given frequency in compared with an impedance analyzer. The frequency behavior of the C^4D response recorded by a detection circuitry depends on both of that of C^4D and the circuitry. Because of the difference in the design of detection circuitry and the dimension of C^4D, the optimization of operating frequency for maximum sensitivity is related to the experimental conditions.

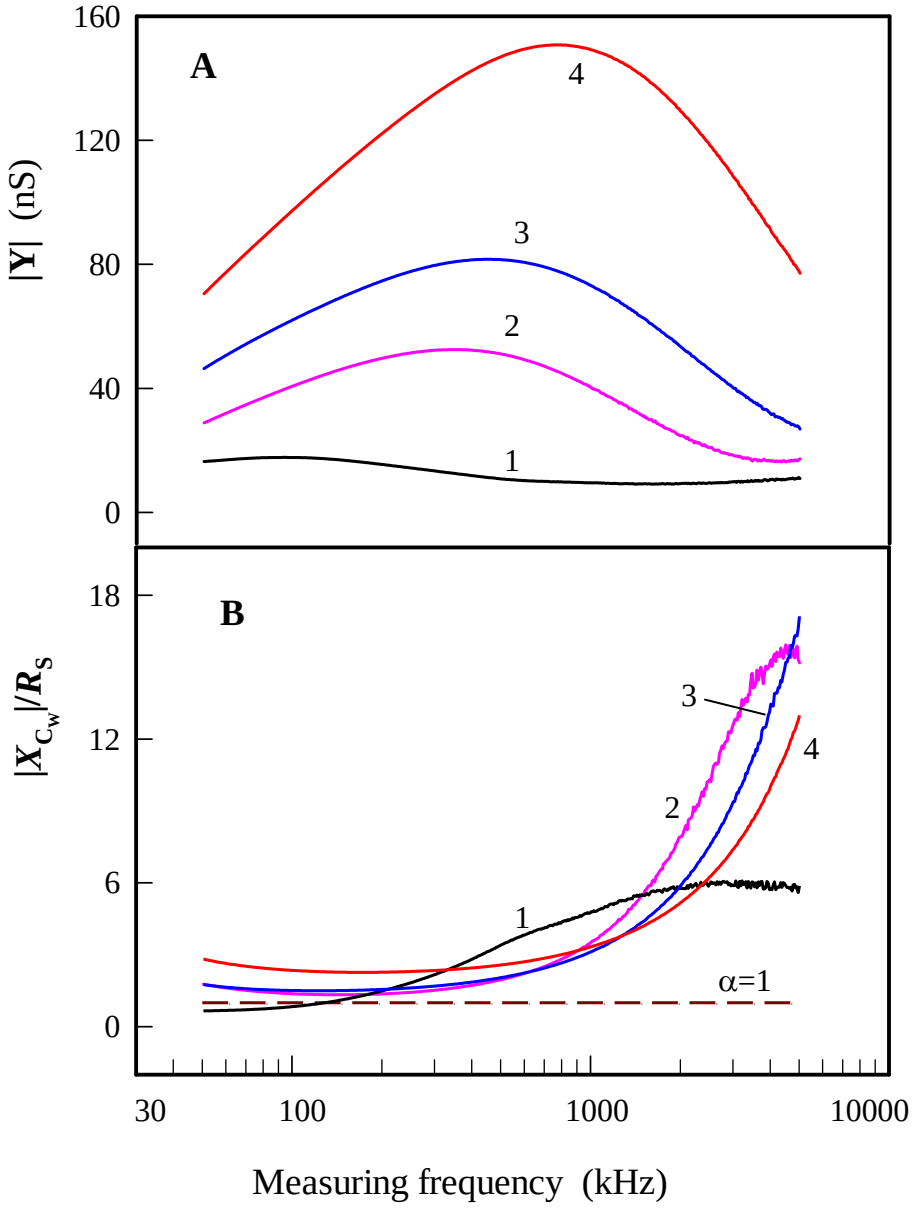

Figure 8. Influence of the measuring frequency on the admittance magnitude (A) and the ratio of reactance of wall capacitance to solution resistance (B) of C^4D. Other experimental conditions: L=18 mm,d =1.1 mm. KCl concentration: (1): 1 mM; (2): 5 mM; (3): 10 mM; (4): 30 mM.

4. CONCLUSION

An impedance analysis method was employed to measure the equivalent circuit parameters of C^4D in capillary electrophoresis. The change in the parameters was analyzed by an electrical line distribution model. As the electrical lines from the electrode to solution are not perpendicular to the capillary, the wall capacitance is much less than the prediction from a cylinder capacitor model. With

increasing solution conductivity, the value of wall capacitance and the length of detection zone increase, the cell constant of the detector decreases. With increasing electrode length, C_w and R_s increase and attain plateau values. Only part of the liquid in capillary within the electrode takes part in the conducting of signal current. As the electrode gap size and operating frequency increase, the values of C_W and R_S reduce. A maximum admittance magnitude was observed on the frequency dependent curve. It was shown that the total impedance of a C^4D under capillary electrophoresis conditions is composed mainly by the impedance from the wall capacitor. The response of C^4D is due to the change in both of C_W and R_S.

ACKNOWLEDGEMENTS

This work was financially supported by the National Natural Science Foundation of China (No.20975062, 21175084, 21275091) ,the Opening Fund of Key Laboratory of Chemical Biology and Traditional Chinese Medicine Research (Hunan Normal University), Ministry of Education (KLCBTCMR2001-01) and Research Fund for the Doctoral Program of Higher Education of China (No. 20113704110003)

References

1. A.J. Zemann, E. Schnell and D. Volgger, *Anal. Chem.*,70(1998)563.
2. J.A.F. da Silva and C.L. do Lago, Anal. Chem. 1998, 70(1998)4339.
3. M. Pumera, *Talanta*, 74 (2007)358.
4. P. Kubáň and P.C. Hauser, *Anal. Chim. Acta* ,607 (2008)15.
5. P. Kubáň and P.C. Hauser, *Electrophoresis*, 30(2009)176.
6. A.A. Elbashir and H.Y. Aboul-Enein, *Biomed. Chromatogr.*,24(2010)1038.
7. P. Kubáň and P.C. Hauser, *Electrophoresis*, 32(2011)30.
8. W.K.T. Coltro, R.S. Lima, T.P. Segato, E. Carrilho, D.P. de Jesus, C.L. do Lago and J. A. F. da Silva, *Anal. Methods*, 4(2012)25.
9. P. Kubáň and P.C. Hauser, *J. Chromatogr. A*, 1128 (2006)97.
10. E. Gillespie, D. Connolly, M. Macka, P. Hauser and B. Paull, *Analyst*, 133(2008)1104.
11. P. Kubáň, M.A. Müri and P. C. Hauser, Analyst, 129(2004)82.
12. E. Gillespie, D. Connolly, M. Macka, P.N. Nesterenko and B. Paull, Analyst, 132 (2007)1238.
13. A. Makahleh and B. Saad, *Anal. Chim. Acta*, 694 (2011)90.
14. E. Gillespie, D. Connolly, P.N. Nesterenko and B. Paull, Analyst, 133(2008)874.
15. D. Connolly, P. Floris, P.N. Nesterenko and B. Paull, *Trends Anal. Chem.*, 29(2010)870.
16. R.M. Saito, C.An. Neves, F.S. Lopes, L. Blanes, J.G.A. Brito-Neto and C.L. do Lago, *Anal.* Chem.,79(2007)215.
17. B.P.Cahill, R. Land, T. Nacke, M. Min and D. Beckmann, *Sens. Actuators B*, 159, (2011)286.
18. B. Gaš, J. Zuska, P. Coufal and T. van de Goor, *Electrophoresis*, 23(2002)3520.
19. S.E. Johnston, K.E. Fadgen, L.T. Tolley and J.W. Jorgenson, *J. Chromatogr. A*, 1094 (2005)148.
20. J.F. da Silva, N. Guzman and C.L. do Lago, *J. Chromatogr. A*, 942 (2002)249.
21. P. Kubáň and P.C. Hauser, *Electrophoresis*, 25 (2004)3387.
22. J.A. Brito-Neto, J.F. da Silva, L. Blanes and C.L. do Lago, *Electroanalysis*,17(2005)1198.
23. J. Tanyanyiwa, B. Galliker, M. A. Schwarz and P. C. Hauser, *Analyst*, 127(2002) 214.
24. P. Tůma, F. Opekar and K. Štulík, *Electrophoresis*, 23(2002)3718.
25. P.Tůma, E. Samcová and K. Štulík, *Electroanalysis*,21(2009)590.
26. P. Kubáň and P.C. Hauser, *Electrophoresis*, 25(2004)3398.

27. J.A. Brito-Neto, J.F. da Silva, L. Blanes and C.L. do Lago, Electroanalysis, 17(2005)1207.
28. K. J.M. Francisco and C. L. do Lago, *Electrophoresis*, 30(2009)3458.
29. E. Baltussen, R. M. Guijt, G. van der Steen, F. Laugere,S. Baltussen and G. W. K. van Dedem,*Electrophoresis*, 23(2002)2888.
30. A. J. Zemann, *Electrophoresis*, 24(2003)2125.
31. C. G. Chen, L. G. Li, Y. J. Si and Y. P. Li, *Electrochim. Acta*, 54(2009)6959.
32. W. K. T. Coltro, J. A. F. da Silva and E. Carrilho, *Electrophoresis*,29(2008)2260.
33. C.Y. Lee,C. M. Chen,G.L. Chang, C.H. Lin and L.M. Fu, *Electrophoresis*, 27(2006) 5043.